

AEROSOL RESEARCH LETTER

# Chemical Smoke Marker Emissions During Flaming and Smoldering Phases of Laboratory Open Burning of Wildland Fuels

Taehyoung Lee,<sup>1</sup> Amy P. Sullivan,<sup>1</sup> Laura Mack,<sup>1</sup> Jose L. Jimenez,<sup>2</sup> Sonia M. Kreidenweis,<sup>1</sup> Timothy B. Onasch,<sup>3</sup> Douglas R. Worsnop,<sup>3</sup> William Malm,<sup>4</sup> Cyle E. Wold,<sup>5</sup> Wei Min Hao,<sup>5</sup> and Jeffrey L. Collett, Jr.<sup>1</sup>

<sup>1</sup>*Atmospheric Science Department, Colorado State University, Fort Collins, Colorado, USA*

<sup>2</sup>*Department of Chemistry and Biochemistry and CIRES, University of Colorado, Boulder, Colorado, USA*

<sup>3</sup>*Aerodyne Research Incorporated, Billerica, Massachusetts, USA*

<sup>4</sup>*National Park Service/CIRA, CSU, Fort Collins, Colorado, USA*

<sup>5</sup>*USDA/FS Fire Science Laboratory, Missoula, Montana, USA*

[Supplementary materials are available for this article. Go to the publisher's online edition of *Aerosol Science and Technology* to view the free supplementary files.]

## 1. INTRODUCTION

Smoke emitted by prescribed and wild fires can make a substantial contribution to ambient aerosol (McMeeking et al. 2006; Park et al. 2007; Spracklen et al. 2007). Approaches to investigate these contributions have used a variety of different chemical smoke markers, including levoglucosan, produced by thermal degradation of cellulose, and water-soluble potassium (Andreae 1983; Engling et al. 2006; Hays et al. 2002; Simoneit 2002; Ward et al. 2006). Filter sampling is commonly employed to measure smoke markers in ambient and source samples; however, these time-integrated measurements limit knowledge about variability of smoke marker emissions, especially between flaming and smoldering fire phases.

Recently developed instruments, such as the Aerodyne High-Resolution Time-of-Flight Aerosol Mass Spectrometer (HR-AMS, AMS hereinafter for short), allow aerosol composition measurements with time resolution of seconds (Canagaratna et al. 2007; DeCarlo et al. 2006). Fragments with mass-to-charge ( $m/z$ ) ratios of 60.021 ( $C_2H_4O_2^+$ ) and 73.029

( $C_3H_5O_2^+$ ) have been suggested as AMS biomass burning markers (Alfarra et al. 2007; Mohr et al. 2009; Schneider et al. 2006). Weimer et al. (2008) reported quadrupole AMS observations of primary smoke particles from flaming and smoldering phases of domestic wood burning. In this article, AMS data are used for the first time to examine key smoke markers emitted during the flaming and smoldering phases from open burning of numerous wildland fuel types. Key AMS smoke marker data presented include  $m/z$  38.964 and  $m/z$  60.021 (referred to as  $K^+$  and  $C_2H_4O_2^+$  hereafter). We also compare  $C_2H_4O_2^+$  measured by the AMS to concentrations of anhydrosugars (levoglucosan, mannosan, and galactosan) obtained by analyzing filter samples (Sullivan et al. 2008). Such observations are key to understanding what ambient AMS marker measurements reveal about primary particle contributions from biomass burning.

## 2. INSTRUMENTATION

During the second Fire Lab at Missoula Experiment (FLAME II), small quantities ( $\sim 250$  g) of more than 20 different biomass fuel types were combusted in an "open burning" configuration. More information on the combustion facility, fuels used, types of burns conducted, and chemical analysis of collected filter samples can be found in Sullivan et al. (2008) and McMeeking et al. (2009). The composition of emitted smoke particles was continuously monitored across evolving flaming and smoldering combustion conditions using the AMS, which has been described in detail elsewhere (Canagaratna et al. 2007; DeCarlo et al. 2006). The fuel was burned under a 1.5 m diameter exhaust stack and the smoke forced up the stack to  $\sim 16$  m above ground where emissions cool to near ambient conditions. A high-volume air pump pulled diluted smoke emissions from the

Received 23 February 2010; accepted 7 May 2010.

This work was funded by NPS (CA2380-99001 TO0356), JFSP (05-3-1-06), NSF (ATM-0521643, ATM-0449815), and USEPA (R833747).

Address correspondence to Jeffrey L. Collett, Jr., Atmospheric Science Department 1371, Colorado State University, Fort Collins, CO 80523, USA. E-mail: collett@atmos.colostate.edu

top of the stack to the AMS through a 3.2 cm diameter, 20 m long stainless steel tube. A typical time from biomass combustion to smoke particle analysis by the AMS was  $\sim 30$  s. The “W” ion path was used to provide higher spectral resolution of measured ion fragments. Collected data ( $\sim 30$  s resolution) were analyzed using AMS data analysis software (SQUIRREL and PIKA) (DeCarlo et al. 2006; Sueper 2009). Details about identification and quantification of smoke marker species measured are provided in the online supplemental information.

### 3. RESULTS AND DISCUSSION

Biomass burning emissions of gases and particles depend strongly on the combustion conditions, which can be broadly classified as flaming or smoldering. The combustion conditions can be monitored using the modified combustion efficiency (MCE), a ratio of emitted  $\text{CO}_2$  to the sum of emitted  $\text{CO}_2$  and  $\text{CO}$  (Chen et al. 2007; McMeeking et al. 2009; Yokelson et al. 1997). In this study MCE values larger than 0.9 and less than 0.8 were used to determine a predominance of flaming or smoldering combustion, respectively. An example timeline of MCE and key particle species emissions is provided in the online supplemental information.

#### 3.1. Emission of Primary Smoke Markers

Previous studies have observed that potassium emission is higher in flaming-dominated combustion (e.g., Echalar et al. 1995) and that levoglucosan emissions are higher during lower temperature (smoldering) burns (Shafizadeh 1982). In order to be most useful as a marker for emissions of primary particle mass (or organic aerosol (OA), which often dominates particle mass), an ideal marker would be emitted at a constant ratio to total particle mass (or OA) across combustion phases and for different biomasses.

Ratios of  $\text{K}^+$  and  $\text{C}_2\text{H}_4\text{O}_2^+$  to particle mass measured by the AMS in the flaming and smoldering phases of individual burns are shown in Figure 1a.  $\text{K}^+$  was typically emitted at a higher mass fraction in flaming phase combustion;  $\text{C}_2\text{H}_4\text{O}_2^+$  was emitted at similar ratios to particle mass in flaming and smoldering phases of most burns. These observations are consistent with the poor relationship between potassium and levoglucosan concentrations reported for FLAME filter samples (Sullivan et al. 2008). Further, Sullivan et al. (2008) reported only modest dependence of the ratio of levoglucosan to aerosol organic carbon on fuel type. Together, these observations suggest that levoglucosan and related products are more universal primary smoke markers than potassium, since they do not depend as strongly on fuel type or combustion conditions.

#### 3.2. Relationships between Anhydrosugars, AMS $\text{C}_2\text{H}_4\text{O}_2^+$ , and AMS OA

Levoglucosan is the most abundant thermal breakdown product of cellulose identified in smoke particles. The thermal degradation of cellulose and hemicellulose also produces other an-

hydrosugars, including mannosan, galactosan, arabinosan, and xylosan. Mass fragment  $m/z$  60 is commonly used as a marker for biomass burning in the AMS, where typically one major ion ( $\text{C}_2\text{H}_4\text{O}_2^+$ ) contributes to the observed signal as also observed in this dataset (see the online supplemental information, Figure S1).

Figure 1b presents the correlation between levoglucosan, or levoglucosan + mannosan + galactosan, as determined from filters (Sullivan et al. 2008), with organic-equivalent (Zhang et al. 2005)  $\text{C}_2\text{H}_4\text{O}_2^+$  measured simultaneously by the AMS. Strong correlations are observed, with correlation coefficients ( $R^2$ ) of 0.91 and 0.93, for the relationship with levoglucosan alone or the sum of three anhydrosugar concentrations, respectively. These results, together with the absence of substantial  $\text{C}_2\text{H}_4\text{O}_2^+$  in most other non-biomass burning aerosol types, confirm that  $\text{C}_2\text{H}_4\text{O}_2^+$  is a suitable AMS marker for primary particle emissions from biomass burning. Multiple field studies have shown that  $\text{C}_2\text{H}_4\text{O}_2^+$  is present at a level of  $\sim 0.3\%$  of total OA during periods without biomass burning influence (e.g., Aiken et al. 2009; Docherty et al. 2008). Mohr et al. (2009) found  $\text{C}_2\text{H}_4\text{O}_2^+$  in AMS analysis of meat cooking aerosols and laboratory studies also indicate it can form in AMS analysis of longer chain alkanolic acids. Takegawa et al. (2007) used an AMS to study oxalic acid, several other larger diacids, and glyoxylic acid and found only minor amounts of  $m/z$  60. As Takegawa et al. (2007) discuss, fragmentation patterns in the AMS can differ from standard 70 eV EI spectra due to the higher vaporizer temperature used in the AMS. We hypothesize that the source of the  $\sim 0.3\%$  background  $\text{C}_2\text{H}_4\text{O}_2^+$  in ambient OA is dominated by acid groups from SOA with a minor contribution from other sources such as meat cooking. The general representativeness of this background value should be evaluated in additional studies.

AMS analyses of levoglucosan, mannosan, and galactosan standards in our laboratory reveal that  $\text{C}_2\text{H}_4\text{O}_2^+$  comprises 14.1, 13.8, and 12.1% of the total ion fragment pattern, respectively (Aiken et al. (2009), Schneider et al. (2006), and Alfara et al. (2007) previously reported values of approximately 13%, 12%, and 8% for levoglucosan, respectively). Using this information, and assuming for the moment that no other molecules in the smoke particles generate  $\text{C}_2\text{H}_4\text{O}_2^+$ , we can calculate an AMS “anhydrosugar-equivalent mass concentration” (anhyd.-eq. conc.), defined as the sum of the levoglucosan, mannosan, and galactosan concentrations required to produce the observed  $\text{C}_2\text{H}_4\text{O}_2^+$  signal intensity. We calculate the anhyd.-eq. conc. by multiplying the observed  $\text{C}_2\text{H}_4\text{O}_2^+$  mass concentration by 7.5 to account for the full anhydrosugar fragment pattern. The results of these calculations are shown in Figure 1c, where the anhyd.-eq. conc. is plotted vs. the sum of the three anhydrosugar concentrations from simultaneous filter samples. If levoglucosan, mannosan, and galactosan were the only molecules in the smoke particles to yield  $\text{C}_2\text{H}_4\text{O}_2^+$ , we would expect the anhyd.-eq. conc. to equal the concentration sum of these three species. Clearly this is not the case. The slope of a best fit line for this dataset is 8.5 with a small intercept, indicating that the AMS  $\text{C}_2\text{H}_4\text{O}_2^+$

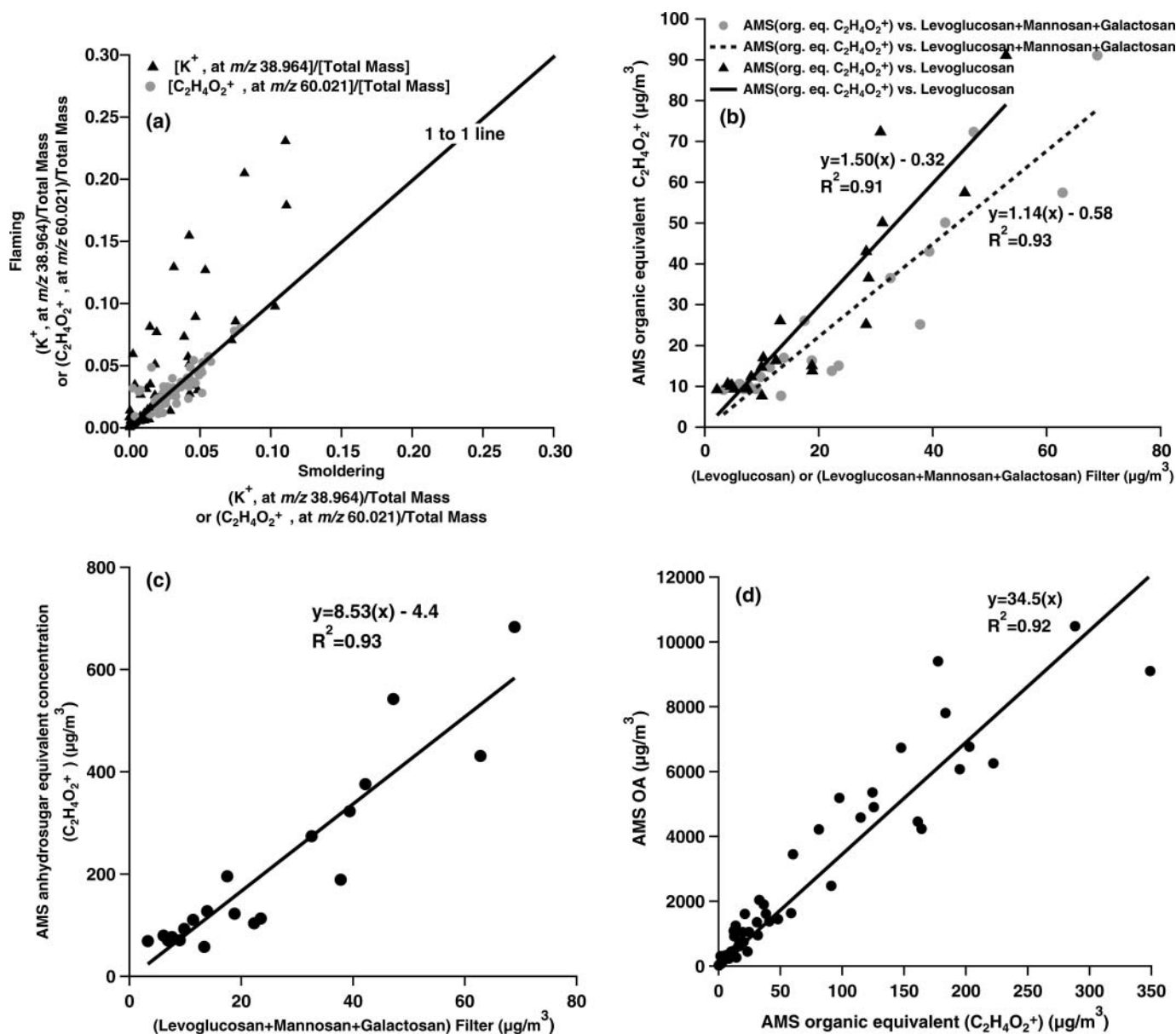


FIG. 1. Observations of smoke particles during FLAME II open biomass burning experiments: (a) comparisons of the ratios of  $K^+$  (at  $m/z$  38.964) and  $C_2H_4O_2^+$  (at  $m/z$  60.021) to total AMS particle mass for flaming and smoldering fire phases of individual FLAME II burns; (b) relationship of organic equivalent concentrations of  $C_2H_4O_2^+$  from the AMS to the concentration of levoglucosan or the concentration sum of levoglucosan, mannosan, and galactosan measured from simultaneously collected filter samples (Sullivan et al. 2008); (c) a hypothetical computed AMS anhydrosugar-equivalent concentration (determined as 7.5 times AMS  $C_2H_4O_2^+$ ) to levoglucosan + mannosan + galactosan concentrations measured in simultaneously collected filter samples; (d) AMS organic aerosol concentration vs. AMS  $C_2H_4O_2^+$  organic equivalent concentration for individual FLAME II burns. The plotted points in each panel represent the average values measured, typically over several minutes of sampling. The orthogonal distance regression approach was used to compute best fit lines in panels (b)–(d).

signal is much larger than can be explained by the three measured anhydrosugars. This is not surprising. Other structurally similar molecules, which are likely abundant in smoke, also produce  $C_2H_4O_2^+$  upon electron impact fragmentation. AMS laboratory tests reveal, for example, that glucose yields an important fragment at  $C_2H_4O_2^+$ , comprising  $\sim 10\%$  of the total ion fragment pattern.

We can also directly investigate the utility of AMS  $C_2H_4O_2^+$  itself as a smoke marker by examining the correlation between OA and  $C_2H_4O_2^+$  across all FLAME II burns. A correlation of  $R^2 = 0.92$  with a slope of 34.5 between biomass burning OA and  $C_2H_4O_2^+$  was observed (Figure 1d), similar to the relationship determined by Aiken et al. (2009) for mostly unprocessed smoke reaching downtown Mexico City from nearby forest fires.

Alfarra et al. (2007) previously proposed a ratio of 36 for domestic wood burning in Zurich and indicate a ratio of 30 was estimated for summertime biomass (presumably open) burning in the region. Weimer et al. (2007) report a much more variable range of this ratio for their residential wood burning experiments and a tendency for lower OA to  $m/z$  60 ratios during flaming conditions.

The correlation between OA and  $C_2H_4O_2^+$  observed here is stronger than the correlation between FLAME filter-based measurements of levoglucosan and OC ( $R^2 = 0.68$ ) (Sullivan et al. 2008). One possible explanation for the improved relationship is that  $C_2H_4O_2^+$  appears to reflect a broader range of biomass burning molecules than the three anhydrosugars discussed here. The sum of all compounds yielding  $C_2H_4O_2^+$  may define a more constant fraction of emitted fine particle OA than does levoglucosan. As Sullivan et al. (2008) point out, the levoglucosan/OC yield appears to vary across fuel components (e.g., branches, needles/leaves, grasses, etc.) in accordance with changes in the fuel mass fraction of cellulose. The less variable ratio of OA to  $C_2H_4O_2^+$  observed here suggests that increases (decreases) in levoglucosan yield in biomass burning smoke may be offset to some extent by corresponding decreases (increases) in other molecules that also yield  $C_2H_4O_2^+$  in the AMS.

The strength of the OA vs.  $C_2H_4O_2^+$  relationship in fresh smoke across fuel types and combustion conditions offers promise that AMS measurements may be useful for directly estimating contributions of biomass burning primary emissions to ambient fine particle organic carbon. Additional research is necessary, however, to assess this relationship as a function of other biomass burning source types (e.g., residential wood burning) and various atmospheric processes, including smoke dilution (which may affect organic gas-particle partitioning) and smoke plume aging.

## REFERENCES

- Aiken, A., Salcedo, D., Cubison, M. J., Huffman, J. A., DeCarlo, P. F., Ulbrich, I. M., Docherty, K. S., Sueper, D., Kimmel, J. R., Worsnop, D. R., Trimborn, A., Northway, M., Stone, E. A., Schauer, J. J., Volkamer, R. M., Fortner, E., de Foy, B., Wang, J., Laskin, A., Shuthanandan, V., Zheng, J., Zhang, R., Gaffney, J., Marley, N. A., Paredes-Miranda, G., Arnott, W. P., Molina, L. T., Sosa, G., and Jimenez, J. L. (2009). Mexico City Aerosol Analysis During MILAGRO Using High Resolution Aerosol Mass Spectrometry at the Urban Supersite (T0)—Part 1: Fine Particle Composition and Organic Source Apportionment. *Atmos. Chem. Phys.* 9:6633–6653.
- Alfarra, M. R., Prevot, A. S. H., Szidat, S., Sandradewi, J., Weimer, S., Lanz, V. A., Schreiber, D., Mohr, M., and Baltensperger, U. (2007). Identification of the Mass Spectral Signature of Organic Aerosols from Wood Burning Emissions. *Environ. Sci. Technol.* 41:5770–5777.
- Andreae, M. O. (1983). Soot Carbon and Excess Fine Potassium: Long-Range Transport of Combustion-Derived Aerosols. *Science* 220:1148–1151.
- Canagaratna, M. R., Jayne, J. T., Jimenez, J. L., Allan, J. D., Alfarra, M. R., Zhang, Q., Onasch, T. B., Drewnick, F., Coe, H., Middlebrook, A., Delia, A., Williams, L. R., Trimborn, A. M., Northway, M. J., DeCarlo, P. F., Kolb, C. E., Davidovits, P., and Worsnop, D. R. (2007). Chemical and Microphysical Characterization of Ambient Aerosols with the Aerodyne Aerosol Mass Spectrometer. *Mass Spectrom. Rev.* 26:185–222.
- Chen, L. W. A., Moosmuller, H., Arnott, W. P., Chow, J. C., Watson, J. G., Susott, R. A., Babbitt, R. E., Wold, C. E., Lincoln, E. N., and Hao, W. M. (2007). Emissions from Laboratory Combustion of Wildland Fuels: Emission Factors and Source Profiles. *Environ. Sci. Technol.* 41:4317–4325.
- DeCarlo, P. F., Kimmel, J. R., Trimborn, A., Northway, M. J., Jayne, J. T., Aiken, A. C., Gonin, M., Fuhrer, K., Horvath, T., Docherty, K. S., Worsnop, D. R., and Jimenez, J. L. (2006). Field-Deployable, High-Resolution, Time-of-Flight Aerosol Mass Spectrometer. *Anal. Chem.* 78:8281–8289.
- Docherty, K. S., Stone, E. A., Ulbrich, I. M., DeCarlo, P. F., Snyder, D. C., Schauer, J. J., Peltier, R. E., Weber, R. J., Murphy, S. M., Seinfeld, J. H., Grover, B. D., Eatough, D. J., and Jimenez, J. L. (2008). Apportionment of Primary and Secondary Organic Aerosols in Southern California During the 2005 Study of Organic Aerosols in Riverside (SOAR-1). *Environ. Sci. Technol.* 42:7655–7662.
- Echalar, F., Gaudichet, A., and Cachier, H. (1995). Aerosol Emissions by Tropical Forest and Savanna Biomass Burning: Characteristic Trace Elements and Fluxes. *Geophys. Res. Lett.* 22:3039–3042.
- Engling, G., Herckes, P., Kreidenweis, S. M., Malm, W. C., and Collett Jr., J. L. (2006). Composition of the Fine Organic Aerosol in Yosemite National Park During the 2002 Yosemite Aerosol Characterization Study. *Atmos. Environ.* 40:2959–2972.
- Hays, M. D., Geron, C. D., Linna, K. J., Smith, N. D., and Schauer, J. J. (2002). Speciation of Gas-Phase and Fine Particle Emissions from Burning of Foliar Fuels. *Environ. Sci. Technol.* 36:2281–2295.
- McMeeking, G. R., Kreidenweis, S. M., Baker, S., Carrico, C. M., Chow, J. C., Collett, J. L., Hao, W. M., Holden, A. S., Kirchstetter, T. W., Malm, W. C., Moosmuller, H., Sullivan, A. P., and Wold, C. E. (2009). Emissions of Trace Gases and Aerosols During the Open Combustion of Biomass in the Laboratory. *J. Geophys. Res.* 114:D19210.
- McMeeking, G. R., Kreidenweis, S. M., Lunden, M., Carrillo, J., Carrico, C. M., Lee, T., Herckes, P., Engling, G., Day, D. E., Hand, J., Brown, N., Malm, W. C., and Collett Jr., J. L. (2006). Smoke-Impacted Regional Haze in California During the Summer of 2002. *Agr. Forest Meteorol.* 137:25–42.
- Mohr, C., Huffman, J. A., Cubison, M. J., Aiken, A. C., Docherty, K. S., Kimmel, J. R., Ulbricht, I. M., Hannigan, M., and Jimenez, J. L. (2009). Characterization of Primary Organic Aerosol Emissions from Meat Cooking, Trash Burning, and Motor Vehicles with High-Resolution Aerosol Mass Spectrometry and Comparison with Ambient and Chamber Observations. *Environ. Sci. Technol.* 43:2443–2449.
- Park, R. J., Jacob, D. J., and Logan, J. A. (2007). Fire and Biofuel Contributions to Annual Mean Aerosol Mass Concentrations in the United States. *Atmos. Environ.* 41:7389–7400.
- Schneider, J., Weimer, S., Drewnick, F., Borrmann, S., Helas, G., Gwaze, P., Schmid, O., Andreae, M. O., and Kirchner, U. (2006). Mass Spectrometric Analysis and Aerodynamic Properties of Various Types of Combustion-Related Aerosol Particles. *Int. J. Mass Spectrom.* 258:37–49.
- Shafizadeh, F. (1982). Introduction to Pyrolysis of Biomass. *J. Anal. Appl. Pyrol.* 3:283–305.
- Simoneit, B. R. T. (2002). Biomass Burning—A Review of Organic Tracers for Smoke from Incomplete Combustion. *Appl. Geochem.* 17:129–162.
- Spracklen, D. V., Logan, J. A., Mickley, L. J., Park, R. J., Yevich, R., Westerling, A. L., and Jaffe, D. A. (2007). Wildfires Drive Interannual Variability of Organic Carbon Aerosol in the Western US in Summer. *Geophys. Res. Lett.* 34:L16816.
- Sueper, D. (2009). ToF-AMS High Resolution Analysis Software, Online available at <http://cires.colorado.edu/jimenez-group/ToFAMSResources/ToFSoftware/index.html>.
- Sullivan, A. P., Holden, A. S., Patterson, L. A., McMeeking, G. R., Kreidenweis, S. M., Malm, W. C., Hao, W. M., Wold, C. E., and Collett, J. L. (2008). A Method for Smoke Marker Measurements and its Potential Application for Determining the Contribution of Biomass Burning from Wildfires and Prescribed Fires to Ambient  $PM_{2.5}$  Organic Carbon. *J. Geophys. Res.* 113:D22302.
- Takegawa, N., Miyakawa, T., Kawamura, K., and Kondo, Y. (2007). Contribution of Selected Dicarboxylic and W-Oxocarboxylic Acids in Ambient Aerosol to the  $m/z$  44 Signal of an Aerodyne Aerosol Mass Spectrometer. *Aerosol Sci. Technol.* 41:418–437.

- Ward, T. J., Hamilton, R. F., Dixon, R. W., Paulsen, M., and Simpson, C. D. (2006). Characterization and Evaluation of Smoke Tracers in PM: Results from the 2003 Montana Wildfire Season. *Atmos. Environ.* 40: 7005–7017.
- Weimer, S., Alfarra, M. R., Schreider, D., Mohr, M., Prevot, A. S. H., and Baltensperger, U. (2008). Organic Aerosol Mass Spectral Signatures from Wood-Burning Emissions: Influence of Burning Conditions and Wood Type. *J. Geophys. Res.* 113, D10304.
- Yokelson, R. J., Susott, R., Ward, D. E., Reardon, J., and Griffith, D. W. T. (1997). Emissions from Smoldering Combustion of Biomass Measured by oPen-Path Fourier Transform Infrared Spectroscopy. *J. Geophys. Res.* 102:18865–18877.
- Zhang, Q., Alfarra, M. R., Worsnop, D. R., Allan, J. D., Coe, H., Canagaratna, M. R., and Jimenez, J. L. (2005). Deconvolution and Quantification of Hydrocarbon-Like and Oxygenated Organic Aerosols Based on Aerosol Mass Spectrometry. *Environ. Sci. Technol.* 39:4938–4952.

## Supplemental Information for:

### Chemical smoke marker emissions during flaming and smoldering phases of laboratory open burning of wildland fuels

Taehyoung Lee<sup>1</sup>, Amy P. Sullivan<sup>1</sup>, Laura Mack<sup>1</sup>, Jose L. Jimenez<sup>2</sup>, Sonia M. Kreidenweis<sup>1</sup>, Timothy B. Onasch<sup>3</sup>, Douglas R. Worsnop<sup>3</sup>, William Malm<sup>4</sup>, Cyle E. Wold<sup>5</sup>, Wei Min Hao<sup>5</sup>, and Jeffrey L. Collett, Jr.<sup>1</sup>

<sup>1</sup>Department of Atmospheric Science, Colorado State University, Fort Collins, CO 80523

<sup>2</sup>Department of Chemistry and Biochemistry and CIRES, University of Colorado, Boulder, CO 80309

<sup>3</sup>Aerodyne Research Incorporated, Billerica, MA 01821

<sup>4</sup>National Park Service/CIRA, Colorado State University, Fort Collins, CO80523.

<sup>5</sup>USDA/Forest Service Fire Science Laboratory, Missoula, Montana

HR-AMS smoke marker data presented in this study include observations of  $K^+$  ( $m/z$  38.964) and  $C_2H_4O_2^+$  ( $m/z$  60.021). Only one ion ( $C_2H_4O_2^+$ ) is found near  $m/z$  60 as shown in Fig. S1a. Consequently, even unit mass resolution would be adequate to quantify this ion during our source measurements. By contrast,  $m/z$  39 measured at unit mass resolution would contain contributions from both  $K^+$  ( $m/z$  38.964) and  $C_3H_3^+$  (39.023) as shown in Fig. S1b. Accordingly, the high resolution provided by the HR-AMS is needed to clearly separate and quantify contributions from these two fragments.

One complication with potassium measurement in the AMS is its tendency to volatilize slowly at the temperature of the AMS vaporizer. While AMS data processing of most peaks corrects for background interference by subtracting the ion signal when the particle beam chopper is closed from the signal when the beam chopper is in the open position, this proves not to be appropriate for quantifying  $K^+$ . This is consistent with the detection of other low-volatility species, such as particulate Pb, with the AMS (Huffman et al., 2009; Salcedo et al., 2010). As observed in the “open” and “closed” panels of Fig. S1b and the time series of  $K^+$  in Fig. S2, a substantial fraction of the  $K^+$  signal is observed after the chopper blocks the aerosol. This is quite different than observed for most other peaks (e.g., the  $C_2H_4O_2^+$  ion shown in Fig. S1a). In order to account for slow vaporization of potassium, quantification of  $K^+$  was determined based on a corrected version of the AMS  $K^+$  difference signal (the difference between open- and closed- beam measurements). The time-resolved difference signal was multiplied by a burn-averaged correction factor to compensate for the delay between particle collection and  $K^+$  ion observation resulting from slow vaporization. In cases where volatilization is slow, both electron impact ionization and surface ionization (on the heated vaporizer) may contribute to the observed ion signal. Since the  $K^+$  peaks observed here exhibit shapes similar to peaks from other ions

produced by electron impact ionization and the  $m/z$  value of the peak closely matches the expected value, the AMS PIKA software provides a reasonable fit to the observed peak and it appears that surface ionization makes, at most, a small contribution to the observed signal. Nevertheless we conservatively interpret the absolute amounts of potassium reported here as approximate. The fact that the reported absolute  $K^+$  concentration values may exhibit some bias, however, does not preclude a comparison of the relative amounts of  $K^+$  observed in flaming and smoldering phases, the main objective of our analysis for this species.

The modified combustion efficiency (MCE) can provide convenient insight into fire phase. High MCE values, typically well above 0.9, indicate efficient combustion associated with a flaming fire; MCE values for smoldering combustion are typically in the 0.7-0.9 range (Chen et al., 2007). Similar values were observed during the FLAME experiments for flaming and smoldering phases. Visual observations during FLAME indicated that many burns underwent a transition phase, where parts of the fuel bed were flaming while other parts were smoldering. Chen et al. (2007) reported similar observations of transitions in their earlier open burning experiments. In order to limit inclusion of these complex heterogeneous combustion periods in our analysis, we examined flaming emissions only when MCE exceeded 0.9 and smoldering emissions for MCE less than 0.8. By combining measurements from the HR-AMS and continuous gas monitors, we can gain insight into changes in biomass burning emissions as individual fires transition from flaming to smoldering conditions. Figure S3 provides one example of such observations. MCE begins high and then drops rapidly midway through the experiment, indicating the transition from flaming to smoldering conditions. Two distinct periods of high particle emissions are observed, one during the flaming part of the fire and another following the transition to smoldering conditions. Substantial emissions of organic aerosol and  $C_2H_4O_2^+$  are observed during both the flaming and smoldering portions of the fire, while  $K^+$  emissions in this example are associated mainly with flaming conditions. The flaming and smoldering fire phases, so apparent in this example of black spruce combustion, were not always so nicely separated in other burns.

Organic fragment concentrations are presented in the manuscript as organic-equivalent concentrations (org.-eq. conc.) (Zhang et al., 2005). The org.-eq. conc. is obtained by dividing the nitrate-equivalent concentration obtained based on the nitrate ionization efficiency calibration from the AMS (Jimenez et al., 2003) by the relative ionization efficiency of organics vs. nitrate. Zhang et al. (2005) report good agreement between total AMS organic concentrations obtained using this approach and independent measurements of organic carbon using a Sunset Laboratories OC/EC analyzer, and Canagaratna et al. (2007) summarize similar results from other studies.

## REFERENCE

Canagaratna, M. R., Jayne, J. T., Jimenez, J. L., Allan, J. D., Alfarra, M. R., Zhang, Q., Onasch, T. B., Drewnick, F., Coe, H., Middlebrook, A., Delia, A., Williams, L. R., Trimborn, A. M., Northway, M. J., DeCarlo, P. F., Kolb, C. E., Davidovits, P. and Worsnop, D. R. (2007). Chemical and microphysical characterization of ambient aerosols with the aerodyne aerosol mass spectrometer. *Mass Spectrom. Rev.* 26:185-222.

- Chen, L. W. A., Moosmueller, H., Arnott, W. P., Chow, J. C., Watson, J. G., Susott, R. A., Babbitt, R. E., Wold, C. E., Lincoln, E. N. and Hao, W. M. (2007) Emissions from laboratory combustion of wildland fuels: emission factors and source profiles. *Environ. Sci. Technol.* 41: 4317-4325.
- Huffman, J.A., Docherty, K. S., Aiken, A. C., Cubison, M. J., Ulbrich, I. M., DeCarlo, P. F., Sueper, D., Jayne, J. T., Worsnop, D. R., Ziemann, P. J. and Jimenez, J. L. (2009) Chemically-resolved aerosol volatility measurements from two megacity field studies. *Atmos. Chem. Phys.* 9:7161-7182.
- Jimenez, J. L., Jayne, J. T., Shi, Q., Kolb, C. E., Worsnop, D. R., Yourshaw, I., Seinfeld, J. H., Flagan, R. C., Zhang, X., Smith, K. A., Morris, J. and Davidovits, P. (2003) Ambient Aerosol Sampling with an Aerosol Mass Spectrometer. *J. Geophys. Res.*, 108, 8425, doi:10.1029/2001JD001213, 2003.
- Salcedo, D., Onasch, T. B., Aiken, A. C., Williams, L. R., de Foy, B., Cubison, M. J., Worsnop, D. R., Molina, L. T. and Jimenez, J. L. (2010) Determination of particulate lead during MILAGRO / MCMA-2006 using Aerosol Mass Spectrometry. *Atmos. Chem. Phys. Disc.* 10:2581-2632.
- Zhang, Q., Alfarra, M. R., Worsnop, D. R., Allan, J. D., Coe, H., Canagaratna, M. R. and Jimenez, J. L. (2005). Deconvolution and quantification of hydrocarbon-like and oxygenated organic aerosols based on aerosol mass spectrometry. *Environ. Sci. Technol* 39:4938-4952.



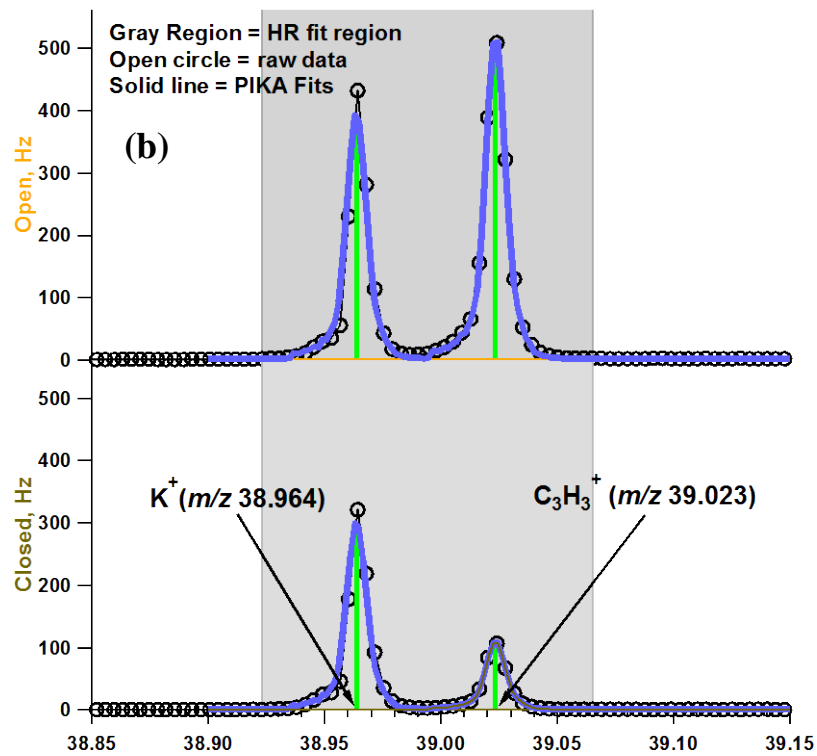
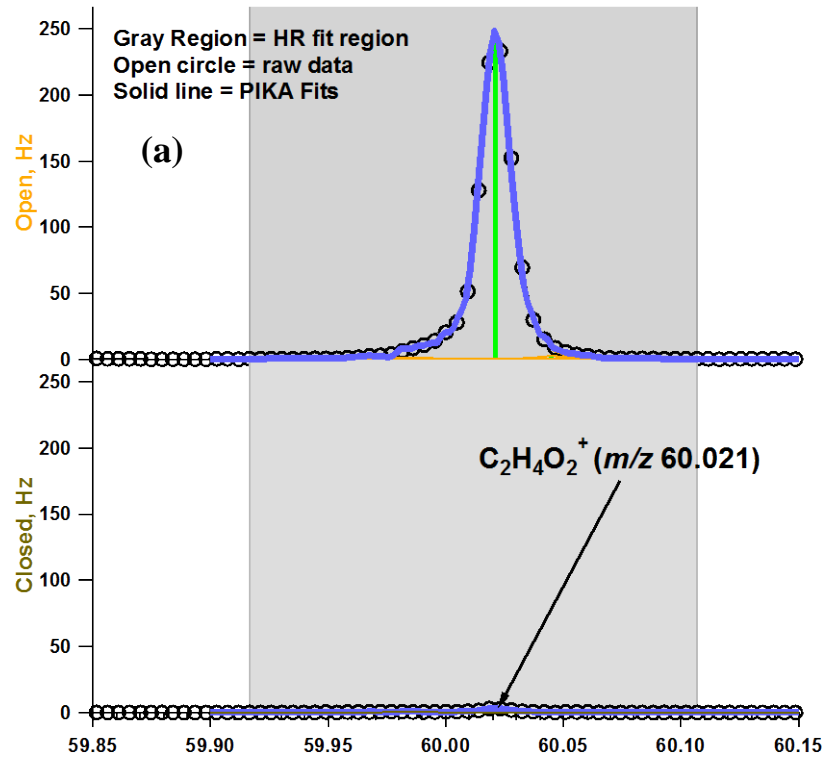


**Figure S1.** HR sticks and PIKA HR fits for (a)  $C_2H_4O_2^+$  at  $m/z$  60 and (b)  $K^+$  and  $C_3H_3^+$  at  $m/z$  39 for HR-AMS measurement of smoke particles from a burn of dry black spruce.

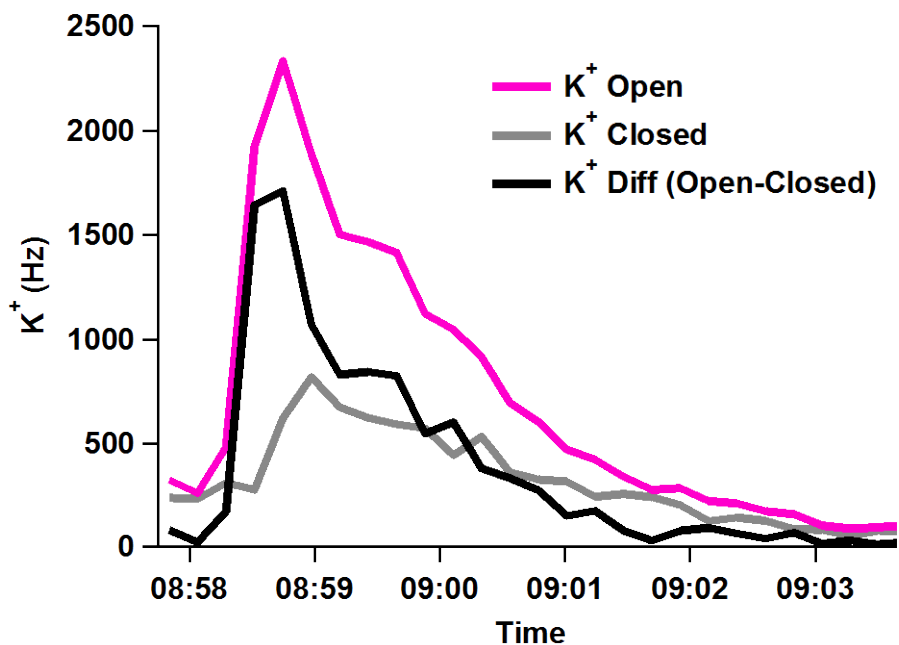


**Figure S2.** Time-resolved signals of  $K^+$  ( $m/z$  38.964) observed in open- and closed-beam portions of the AMS measurement cycle, and their difference, during measurement of smoke particle emissions from a burn of dry black spruce.

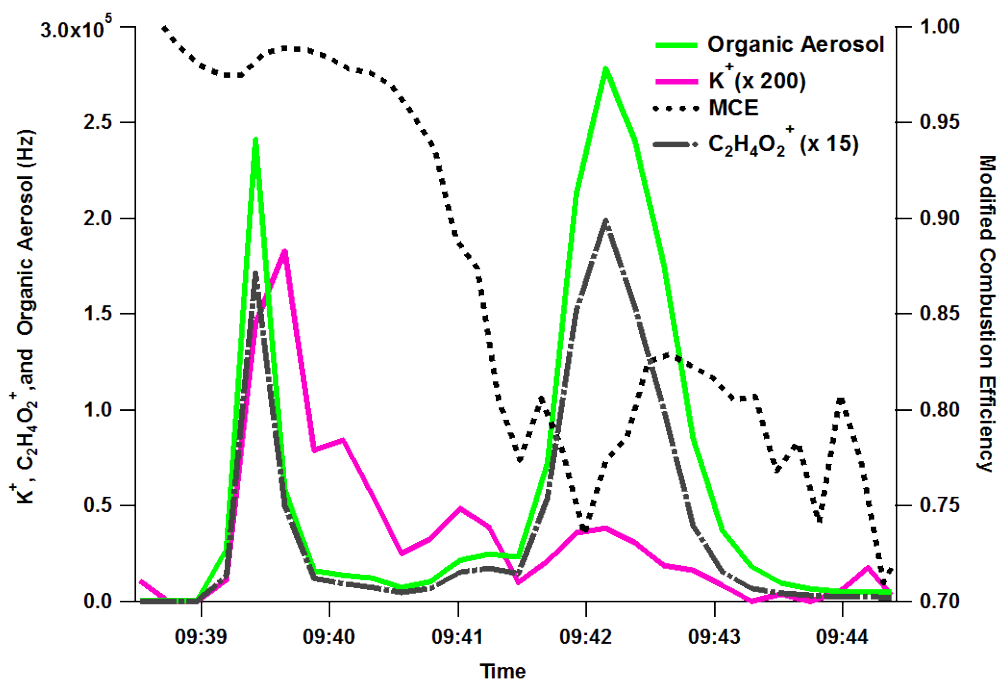


**Figure S3.** Modified combustion efficiency and concentrations of organic aerosol,  $K^+$  ( $m/z$  38.964), and  $C_2H_4O_2^+$  ( $m/z$  60.021) from HR-AMS measurements during a burn of fresh black spruce.